periment tends to confirm these features of the calculation. The absolute magnitude of the theoretical cross section is 25% larger than experiment at low velocity, and this discrepancy decreases at higher velocities. The magnitude of the cross section depends on the difference potential for large internuclear separation $R > 10a_0$. The relative accuracy of the difference potential is less at large R where the difference potential is small. The uncertainty in ΔV at $R = 15a_0$ is $\pm 10\%$, and the uncertainty in the theoretical cross section is $\pm 5\%$. The stated experimental uncertainty is $\pm 15\%$. Michels's potential, which is considerably smaller than ours for large R, yields a cross section whose magnitude is in good agreement with experiment.

VIII. CONCLUSIONS

To review, we have set up a one-electron effective Hamiltonian for Li_2^+ and have found the six lowest eigenvalues as a function of internuclear separation. The numerical method used is economical and accurate and may find application in other one-electron problems. The intermolecular potentials, together with one matrix element, were used to calculate absolute cross sections for three scattering processes which have been measured. Qualitatively, the theoretical model explains all the observed features of the cross sections. In particular, the observed level crossing[1] is identified as a crossing of the σ_{u1} and π_{u1} levels. Where a quantitative comparison is possible, the calculated cross sections agree with experiment within the author's assessment of possible experimental error. There are sound theoretical reasons for believing that the theoretical model, simple though it is, is an accurate physical model for Li_2^+ for $R > 2a_0$. It is therefore desirable to have accurate experimental measurements to test the theory. It is desirable to have (a) absolute elastic cross sections over a wider range of energies with a careful study of the interference term, (b) absolute inelastic cross sections in order to compare the magnitude and shape of the curves, and (c) a more accurate absolute measurement of the charge-transfer cross section.

The theoretical methods used here can be applied to the other symmetric or asymmetric alkali molecular ions and to the alkali-hydride molecular ions.

[1]W. Aberth, O. Bernardini, D. Coffey, Jr., D. C. Lorents, and R. E. Olson, Phys. Rev. Letters 24, 345 (1970).
[2]D. C. Lorents, G. Black, and O. Heinz, Phys. Rev. 137, A1049 (1965).
[3]J. Perel, H. L. Daley, J. M. Peek, and T. A. Green, Phys. Rev. Letters 23, 677 (1969).
[4]H. S. W. Massey and R. A. Smith, Proc. Roy. Soc. (London) A142, 142 (1933).
[5]K. W. Ford and J. A. Wheeler, Ann. Phys. (N. Y.) 7, 259 (1959).
[6]R. P. Marchi and F. T. Smith, Phys. Rev. 139, A1025 (1965).
[7]C. E. Moore, *Atomic Energy Levels*, Natl. Bur. Std. (U.S.) Circ. No. 467 (U.S. GPO, Washington, D. C., 1949).
[8]J. C. Slater, Phys. Rev. 32, 349 (1928).
[9]C. R. Fischer and P. J. Kemmey, Phys. Rev. 186, 272 (1969).
[10]F. T. Smith, R. P. Marchi, and K. G. Dedrick, Phys. Rev. 150, 79 (1966).
[11]D. R. Bates and D. A. Williams, Proc. Phys. Soc. (London) 83, 425 (1964).
[12]J. M. Peek, T. A. Green, J. Perel, and H. M. Michels, Phys. Rev. Letters 20, 1419 (1968).
[13]J. Perel, Phys. Rev. A 1, 369 (1970).
[14]O. B. Firsov, Zh. Eksperim. i Teor. Fiz. 21, 1001 (1951).

PHYSICAL REVIEW A VOLUME 4, NUMBER 1 JULY 1971

Fine Structure and Diamagnetic Zeeman Effect in He ($4\,^3P$)

T. A. Miller and R. S. Freund
Bell Telephone Laboratories, Murray Hill, New Jersey 07974
(Received 16 September 1971)

The $4\,^3P$ state of helium has been excited and aligned by electron impact in a strong magnetic field. Transitions between Zeeman levels of the fine-structure states are induced by microwave frequency radiation and are detected through the resulting change in polarization of 3188-Å fluorescence. The derived values of the fine-structure intervals are $4\,^3P_0$-$4\,^3P_1$ $= 3306.6 \pm 1.0$ MHz and $4\,^3P_1$-$4\,^3P_2 = 270.7 \pm 0.8$ MHz. The diamagnetic Zeeman interaction produces an observable effect, and the magnitude of its anisotropic part has been measured. The atomic radius and quadrupole moment are derived from this measurement and agree within experimental error with the values for a hydrogenic $4p$ orbital.

I. INTRODUCTION

Accurate measurements of the fine structure of helium $2\,^3P$ and $3\,^3P$ have been carried out for many years,[1–10] both for the purpose of testing higher-order corrections to calculated He wave functions

and with the hope of obtaining an improved value for the fine-structure constant α. Calculations of these fine-structure intervals have agreed with experiment to about 100 ppm,[10–14] and efforts are continuing to improve the accuracy of both the calculations[14] and experiments.[8]

The only measurements of fine structure in other states of helium have been by Galleron-Julienne and Descoubes[5(a)] and Maujean and Descoubes.[5(b)] By means of the level-crossing method they have obtained data for the $4\,^3P$-$9\,^3P$, $3\,^3D$-$7\,^3D$, and $5\,^3F$ states. There have been no reported calculations of the fine structure in these other states.

The present study was initiated primarily to test apparatus designs which can be used for microwave frequency spectroscopy of molecules. It quickly became apparent that the data on helium $4\,^3P$ could provide more accurate fine-structure values than the published ones.[5] Our experiment gives a value for the $4\,^3P_1$-$4\,^3P_2$ separation which agrees with that of Galleron-Julienne and Descoubes[5(a)] with experimental error, but disagrees with the later value of Maujean and Descoubes.[5(b)] Our value for the $4\,^3P_0$-$4\,^3P_1$ separation is about two orders of magnitude more precise than either of the previous values.[5]

An unanticipated observation has been that the diamagnetic Zeeman interaction (the $\vec{A}^2$ term in the Hamiltonian) has an observable effect on our transition frequencies. This interaction has not been observed in previous rf studies of paramagnetic atoms since its magnitude increases rapidly with increasing atomic radius and magnetic field, whereas the measurements have been made on atomic states with low principal quantum number or have used low magnetic fields.

The $\vec{A}^2$ term gives rise to both an isotropic shift that is independent of the Zeeman (M) state and an additional anisotropic shift that is different for states of different M (see Sec. II). The M-independent shift is related to the isotropic bulk magnetic susceptibility which has been measured often for atoms and molecules. The M-dependent effect is related to the anisotropy of the diamagnetic susceptibility and to the quadrupole moment of the atom or molecule.

Several optical absorption spectra of the alkali atoms at high magnetic field (~25 000 G) have revealed the effects of the $\vec{A}^2$ term on high Rydberg states (n between 15 and 35).[15–17] It is likely that optical spectra at megagauss magnetic fields will also display this interaction. A recent observation of the sodium D lines at megagauss fields[18] showed a 164-Å first-order Zeeman shift, but because of experimental limitations it was impossible to measure the expected 1.75-Å diamagnetic Zeeman shift. Flygare and co-workers[19] have presented a series of measurements of the anisotropy of the magnetic susceptibility in diamagnetic molecules and of the molecular quadrupole moments. The first measurement of an atomic quadrupole moment has recently been reported[20] for the ground ^2P state of aluminum. Our measurements on the $4\,^3P$ state of helium appear to give the first experimental determination of a quadrupole moment for an excited atomic state.

II. THEORY

The effective Hamiltonian relevant to this problem is

$$\mathcal{H} = \mathcal{H}_{FS} + g_L \mu_B \vec{H}\cdot\vec{L} + g_S \mu_B \vec{H}\cdot\vec{S} + \mathcal{H}_d' , \tag{1}$$

where μ_B is the Bohr magneton, 1.399 60 MHz/G, $\vec{H}$ is the magnetic field, $\vec{L}$ is the electronic orbital angular momentum, and $\vec{S}$ is the total electronic spin angular momentum.

$\mathcal{H}_{FS}$ is the fine-structure Hamiltonian, which consists primarily of terms due to the spin-orbit and spin-spin interactions. In this experiment, which measures the two fine-structure intervals, $4\,^3P_2$-$4\,^3P_1$ (called $\Delta\nu_{12}$) and $4\,^3P_1$-$4\,^3P_0$ (called $\Delta\nu_{01}$), we treat the splittings phenomenologically and do not consider their origins.

The orbital g value g_L is equal to unity, except for higher-order corrections.[6,9,21,22] Explicitly,

$$g_L = 1 + \Delta g_m + \Delta g_r . \tag{2}$$

Δg_m which arises because of the finite nuclear mass, takes the form

$$\Delta g_m = -\,(m/M)\,(1 + \langle B_z\rangle/L_z), \tag{3}$$

where

$$\langle B_z\rangle = \hbar^{-1}\,\langle (\vec{r}_1\times\vec{p}_2)_z + (\vec{r}_2\times\vec{p}_1)_z\rangle , \tag{4}$$

m is the electronic mass, M is the nuclear mass, $\vec{r}_i$ the radius vector of electron i, and $\vec{p}_i$ the momentum of electron i. An approximate calculation using hydrogenic orbitals shows that the second term in Eq. (3) contributes less than 10 ppm for any $n\,^3P$ state with $n > 2$. Δg_r results from several relativistic effects. Since the speed of an np electron decreases as n increases, the relativistic corrections also decrease. Rough calculations show that $\Delta g_r < 10$ ppm for $n\,^3P$ states with $n > 2$.

We have set g_S, the electronic spin g value, equal to the free-electron value, 2.002 32. The only expected corrections are several relativistic terms, the combined effect of which might change g_S by 2 or 3 units in the fifth decimal place. The frequencies of the observed transitions should be quite insensitive to the value of g_S since all the observed transitions are of the approximate form $\Delta M_S = 0$ (see below) and at the high-field limit, the $\Delta M_S = 0$ transition frequencies are independent of g_S. As expected, least-squares fits to our data in which g_S was treated as a variable parameter did not show a statistically significant deviation from the free-

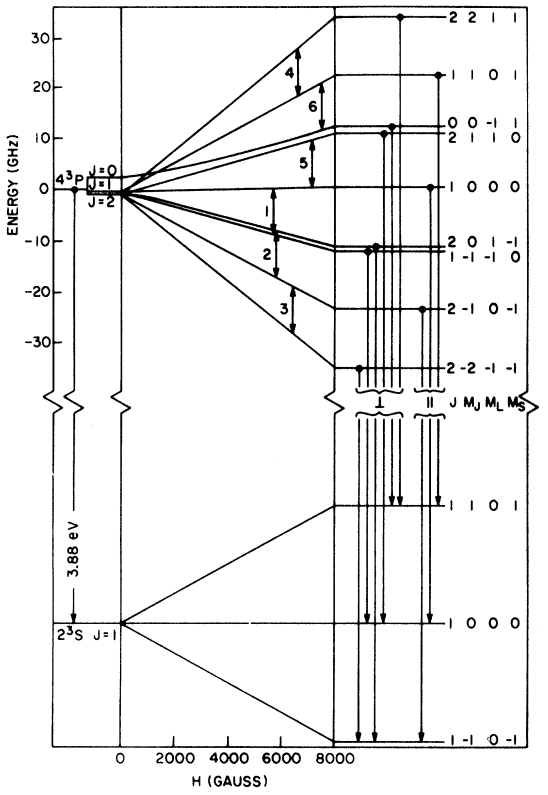

FIG. 1. Energy levels of the helium $4\,^3P$ state (top) and $2\,^3S$ state (bottom) in the presence of a magnetic field. Allowed optical transitions and their polarizations, parallel or perpendicular to the exciting electron beam, are indicated on the right. The only six microwave transitions which are observable in this experiment are numbered in order of increasing magnetic field for fixed frequency.

electron value.

$\mathcal{H}_d'$ is the effective Hamiltonian for the diamagnetic Zeeman interaction within a given electronic state. Its form can be derived from the general diamagnetic interaction,

$$\mathcal{H}_d = \sum_i (e^2/2mc^2)\,\vec{A}_i^2 \,. \tag{5}$$

For a Coulomb gauge and a uniform magnetic field $\vec{A}_i = \frac{1}{2}(\vec{H}\times\vec{r}_i)$ so

$$\mathcal{H}_d = \sum_i (e^2/8mc^2)\,(\vec{H}\times\vec{r}_i)^2 \,. \tag{6}$$

This expression may be rewritten in irreducible tensor form and the operators recoupled so that it can be divided into two parts: one isotropic and the other anisotropic. The energy contribution from the isotropic part is independent of the projection of total angular momentum along $\vec{H}$, and the energy contribution from the anisotropic part gives zero when averaged over all projections:

$$\mathcal{H}_d = -\sum_i \frac{e^2}{4mc^2}\, T^1(\vec{H},\vec{r}_i)\cdot T^1(\vec{H},\vec{r}_i)$$

$$= \sum_i \frac{e^2}{12mc^2}\, H^2\vec{r}_i^{\,2} - \sum_i \frac{e^2}{8mc^2}\, T^2(\vec{H},\vec{H})\cdot T^2(\vec{r}_i,\vec{r}_i) \,. \tag{7}$$

Equation (7) can be rewritten in terms of the usual (isotropic) diamagnetic susceptibility χ_I and its anisotropic analog χ_A by taking the expectation value over the electronic state and using the replacement theorem to replace the second rank tensor in $\vec{r}_i$ by one in $\vec{L}$:

$$\mathcal{H}_d' = -\tfrac{1}{2}\chi_I H^2 - \chi_A\, T^2(\vec{H},\vec{H})\cdot T^2(\vec{L},\vec{L}) \,, \tag{8}$$

where

$$\chi_I = -\sum_i (e^2/6mc^2)\,\langle \eta LM_L |\, \vec{r}_i^{\,2} \,|\eta LM_L\rangle \tag{9}$$

and

$$\chi_A = \sum_i \frac{e^2}{4mc^2L(2L-1)}$$

$$\times \langle \eta LM_L = L \,|\, \vec{r}_i^{\,2}(3\cos^2\theta_i - 1)\,|\eta LM_L = L\rangle \,, \tag{10}$$

where η represents the remaining quantum numbers needed to specify the atomic state.

The energy levels derived from the effective Hamiltonian [Eq. (1)] for helium in the $4\,^3P$ state are shown in Fig. 1. The six observed microwave transitions are indicated.

III. METHOD

The experimental method is similar to that used by Lamb and co-workers.[1-3] A microwave cavity is placed in a strong magnetic field and filled with helium. A beam of electrons, traveling through the cavity along the magnetic field, excites some helium atoms to the $4\,^3P$ state. Because the electrons are moving along a well-defined direction, the excited state of the atom is aligned in the magnetic field, that is, the populations of $M_L = \pm 1$ differ from the population of $M_L = 0$. The subsequent radiation ($4\,^3P \rightarrow 2\,^3S$ at 3188 Å) is polarized (Fig. 1). If microwave radiation at the resonant frequency now interacts with the excited state, the populations of the two connected levels tend to equilibrate and the optical polarization is reduced. Detection of a change in optical polarization, therefore, indicates the occurrence of a microwave transition. Figure 1 illustrates the nine optically allowed transitions in terms of labels appropriate to the high-field limit, $\Delta M_L = 0, \pm 1$ and $\Delta M_S = 0$. Transitions with $\Delta M_L = 0$ are polarized parallel to $\vec{H}$ and those with $\Delta M_L = \pm 1$ are polarized perpendicular. From the diagram it can be seen that only the six indicated microwave transitions lead to the change of polarization required for their observability.

IV. APPARATUS

A. Microwave Cavity

The resonance experiment is carried out in a mi-

crowave cavity, so the available microwave source is able to generate microwave magnetic fields sufficiently intense to give an observable signal. The design of this cavity is based on the following considerations.

High-transition probability with small line broadening is obtained at the "half-saturation power" point, that is, the power for which it is as likely that the atom undergo a microwave transition as an optical transition. Lamb[1] has shown that the amplitude of the microwave magnetic field H_1 required for "half-saturation" is given by

$$H_1 = h/(\tau \mu_B |V|) , \tag{11}$$

where τ is the lifetime of the excited state and V is the magnetic transition moment. In this experiment, the dc magnetic field is sufficiently great that V can be approximated as $1/\sqrt{2}$, its value when the spin and orbital angular moments are completely decoupled. Thus for the $4\,^3P$ He atom with $\tau \sim 150$ nsec, $H_1 \sim 1.1$ G. The average microwave magnetic field $\bar{H}_1$ inside the cavity is approximately related to the power incident upon the cavity by[23]

$$\bar{H}_1 = (1/79.6)(2QP/\mu_0 v\omega)^{1/2} , \tag{12}$$

where Q is the cavity's "figure of merit", v is the volume of the cavity in m^3, ω is 2π times the resonant frequency of the cavity, μ_0 is the permeability of free space, and P is the power (in watts) incident upon the cavity. One sees from Eq. (12) that in order to generate a large $\bar{H}_1$ the cavity should be small and have a high Q.

To carry out the resonance experiment the cavity must have (i) holes for entrance and exit of a beam of electrons traveling parallel to the bulk magnetic field, (ii) a large viewing port to collect 3188-Å radiation from the $4\,^3P$ state, (iii) the microwave magnetic field perpendicular to the bulk magnetic field and the axis of the electron beam, so that transitions may be induced which alter the observed polarization, and (iv) the smallest possible electric field at the location of the electron beam to minimize interaction between the microwaves and the electrons.

These desirable qualities seem best fulfilled in a rectangular resonance cavity operating in the TE_{102} mode. A diagram of this cavity is shown in Fig. 2. Position and size of the electron entrance and exit holes and the viewing port are designed to lower the Q as little as possible. The microwave magnetic field is perpendicular to the electron beam and at a maximum along the beam path while the electric field is zero along this axis. The Q of the cavity is approximately 4000, and its volume is ~ 16 cm^3. Hence, from Eq. (12) the average value of the magnetic field in the cavity is approximately 2 G for 1-W input power. The average field along the beam axis is slightly greater but in any case very little gain in signal strength is noted for incident powers in excess of approximately 2 W. Moreover, for powers above this level, discharges occasionally occur in the cavity. Incident powers below approximately 1–2 W result in loss of signal.

B. Microwave Circuitry

A schematic diagram of the microwave circuit is shown in Fig. 3. Microwaves of a nominal frequency of 9 GHz and power level of approximately 100 mW are delivered by a Varian 153-C klystron. Approximately 1 mW of power is sampled via a directional coupler on the klystron output. This sample power is routed to a Hewlett-Packard model No. 5255 frequency converter and the difference frequency measured by an HP5245L counter. This arrangement permits continuous monitoring of the microwave frequency to an accuracy better than 1 kHz.

The power output of the klystron passes through a 0–50-dB variable attenuator and a fixed gain (approximately 35 dB) traveling wave tube amplifier (Alfred model No. 528). This combination allows a continuously variable microwave power output from approximately 10 mW to about 5 W, the amplifier's saturation point.

From the amplifier the microwaves enter port 1 of a three-port circulator. Port 2 of the circulator is terminated by the microwave cavity, resonant at a nominal frequency of 9 GHz. The fraction of power reflected by the cavity termination (less than 10% of the incident power) emerges from port 3 of the circulator, which is terminated by a 0–30-dB variable attenuator and a crystal detector mount. The variable attenuator serves to protect the crystal detector which plays two important roles in the experiment.

First, the klystron can easily be tuned to the cavity's resonance frequency by monitoring the

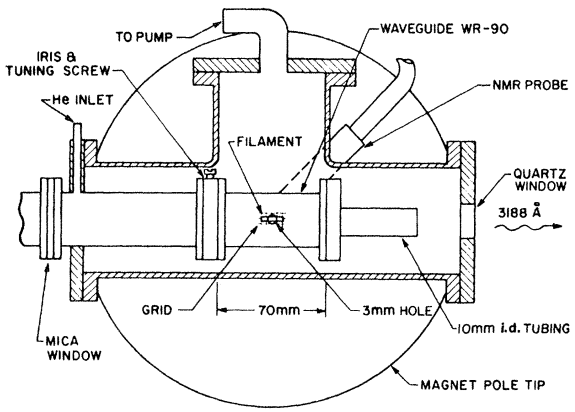

FIG. 2. Diagram of the apparatus, showing the vacuum chamber, microwave cavity, electron gun, and magnet.

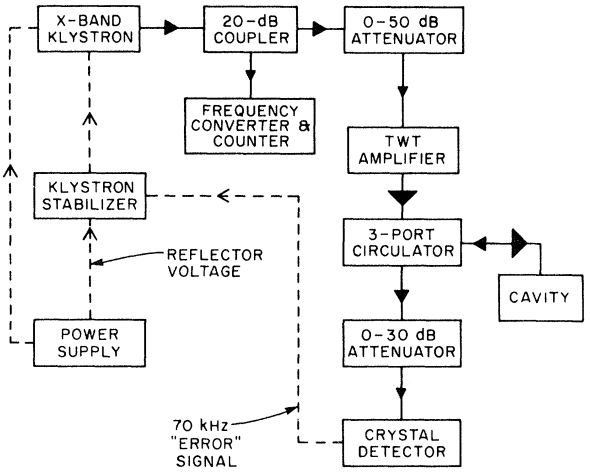

FIG. 3. Microwave circuit.

rectified output voltage of the crystal detector and seeking its minimum. Second, after the cavity's resonance frequency is located, the crystal provides an "error signal" with which the klystron frequency is locked to that of the cavity. This locking is accomplished by a Teltronics klystron stabilizer which provides 70-kHz frequency modulation (of a few kHz amplitude) of the klystron output. At the cavity's resonant frequency, little or no 70-kHz signal reaches the crystal, but a nonresonant microwave frequency produces a 70-kHz error voltage at the crystal, proportional to the deviation from resonance and with a phase characteristic of the sign of this deviation. This signal is applied to the stabilizer which phase detects it and provides the appropriate dc voltage to the reflector of the klystron to bring it into resonance. The ability to lock the klystron to the cavity has been very important for the success of the experiment because both the microwave power dissipated in the walls of the cavity and the electron-gun filament tend to heat the cavity. This heating causes a change in the resonance frequency of the cavity of the order of 5 MHz. The time constant of the cavity to come to a temperature equilibrium is of the order of several hours. Thus through much of the experiment, the cavity drifted at a rate of the order of 10 kHz/min. Had this drift not been constantly compensated for by changes in the klystron frequency, serious microwave power variations would have occurred within the cavity leading to considerable variation in the light output and polarization as well as leading to line-shape distortion.

The microwave power is coupled into the cavity through a capacitive iris and the cavity matched to the transmission line by a brass tuning screw with an enlarged terminal. An earlier attempt to use a nylon tuning screw with a brass stud failed, because sufficient heat was generated by microwave absorption in the brass stud to melt the nylon.

C. Electron Gun

A simple triode electron gun is attached to the outside of the cavity. The cathode is a directly heated platinum filament with an oxide coating.[24] There is a tungsten accelerating grid, and the cavity serves as the anode. Electrons enter the cavity through a 3-mm hole, leave through a 4-mm hole in the far wall and are collected on a separate electrode. Magnetic collimation confines the electron beam to a path defined by the 3-mm hole. The filament is heated by about $3\frac{1}{2}$-A dc. The cathode operates 60–100 V negative with respect to the grounded anode and the collector current is about 200 μA; the precise values are chosen to maximize the resonance signal and are dependent on the helium pressure and the magnetic field. This is because an incipient discharge exists along the electron beam, and the distribution of trapped ions and electrons is very sensitive to these variables.

D. Vacuum Chamber

The vacuum chamber consists of a 2-in. copper plumbing tee with brass flanges. The waveguide which passes through one flange is soft-soldered in place and is vacuum sealed by a mica window. This flange also carries the electrical feed throughs, and the other two flanges carry a window and the pumping connection. All materials were tested and found to be nonmagnetic. An Edwards model No. 450 rotary oil pump with a speed of ~600 liter/min is liquid-nitrogen trapped and pumps on the chamber through a $\frac{1}{2}$-in.-diam tube. Pressure measurement is by a Pirani gauge close to the trap and so is not an accurate indication of the pressure in the cavity. The pressure in the cavity with the filament on but the helium flow off is estimated to be several mTorr.

E. Magnetic Field

A Varian 15-in. magnet is fitted with pole pieces giving a 4-in. airgap. The field uniformity over the volume of luminous helium (which we will call the source) is estimated to be better than 1 part in 10^5. Field strength is measured by an NMR probe which is positioned about 1 in. from the source. The NMR fluxmeter is of the marginal oscillator type and has provision for locking its oscillation frequency to the resonant frequency of the sample. The sample is distilled water doped with 0.02-M $MnSO_4$. Absolute magnetic fields are determined from the NMR frequencies by using a value of $4.257\,59\times10^4$ sec^{-1} G^{-1} for the gyromagnetic ratio of the proton, uncorrected for the diamagnetism of water.

F. Optical

Light emitted by the $4\,^3P$ state passes through (i) a viewing orifice in the end of the cavity, (ii) a fused quartz window, (iii) a sheet of type-HNP'B Polaroid with its polarizing axis parallel to the electron beam, (iv) two fused-quartz lenses, and (v) a 3188-Å interference filter, and is detected by an EMI model No. 6255*SA* photomultiplier. Light emitted by the $3\,^3P$ state is detected without any interference filter, since the 3889-Å line ($3\,^3P \rightarrow 2\,^3S$) contains about $\frac{1}{2}$ the total intensity emitted by helium in the spectral region where the photomultiplier is sensitive. The aperture of the optical system is limited to $f/6$ by the orifice in the cavity. Transmission of the Polaroid is about 30% and of the interference filter, about 15%.

G. Detection

The current from the photomultiplier is measured by a Keithley model No. 610B electrometer with a 10^4-Ω input resistor and the voltage developed across this resistor is fed to a PAR 121 lock-in amplifier. This simple procedure permits measurement of the ac signal with simultaneous monitoring of the dc signal.

The magnetic field is modulated at 100 Hz with an amplitude approximately equal to the linewidth (to obtain maximum sensitivity) by means of coils on the pole tips. A 10-sec time constant is used, except for line No. 6 which requires a 30-sec time constant.

The observed signal-to-noise ratio on most lines is between 2:1 and 5:1. Noise appears to be due basically to statistical fluctuations in the total dc signal (shot noise), but there have been frequent nonrandom bursts two or three times larger. These are probably caused by instabilities in the electron gun.

V. RESULTS

A. Measured Parameters

Each transition was measured at a fixed frequency by sweeping the magnetic field first up and then down through the resonant field and taking the average of the two line centers. Six such measurements were taken for each transition and the average values and standard deviations are given in Table I. Because the microwave frequency drifted between measurements, the six field values were corrected to a common frequency by the relationship

$$\Delta\nu = g\mu_B \Delta H\,, \tag{13}$$

where g is known better than 0.1%. The largest value of $\Delta\nu$ was 0.62 MHz, so the error introduced in the resulting H is certainly negligible.

TABLE I. Observed line positions and residuals from least-squares fit.

Line No.	Frequency (MHz)	H obs (G)	Residual H obs $-H$ calc
1	9006.98	5710.2±0.2	−0.2
2	9007.43	5741.3±0.2	0.0
3	9007.10	6342.2±0.3	0.2
4	9008.25	6534.1±0.3	0.2
5	9008.13	7174.8±0.3	−0.2
6	9007.86	7431.5±0.2	0.0

The four parameters, $\Delta\nu_{01}$, $\Delta\nu_{12}$, g_L, and χ_A were determined by a least-squares fit to the six data points in Table I and are given in Table II. The differences between the observed and the calculated values of H (Table I) are no larger than the measurement error.

B. Error Analysis

The most important source of error is the random measurement error, which is given in Table I as the standard deviation of six measurements of the line position. Systematic errors should also be included in the parameter error estimates. In the remainder of this section, likely systematic errors are examined and shown to be small compared to the random error. Consequently, the error limits reported in Table II are determined entirely by random errors and are chosen as twice the standard error of the parameters.[25]

Magnetic field measurements are based on the NMR probe, which offers precision better than 10 ppm or about 5 mG. There can be, however, a difference in field between the positions of the source and the probe. This difference was found to be less than 100 mG when the field in the magnet gap was mapped with the vacuum chamber removed. The presence of the vacuum chamber might alter this value, however, and the probe cannot be placed inside the assembled apparatus. Hence three transitions (Nos. 1, 2, and 5) in the $3\,^3P$ state of helium were measured and compared to the positions calculated from the data of Wieder and Lamb,[3] with g_L ($3\,^3P$) taken to be $1-(m/M)$. A field-dependent correction to the probe measurements was thereby obtained. The field values for the $4\,^3P$ transitions in Table I include this correction, which ranges from 200 to 400 mG. The remaining error in absolute field measurement is estimated to be less than 50 mG, which is significantly smaller than the measurement error listed in Table I.

A shift of magnetic field might possibly result from the $3\frac{1}{2}$-A current through the heater. We consider this unlikely, since to a first approximation this field is perpendicular to the bulk field and so should have a negligible effect on the magnitude of

the resultant. To check this possibility however several helium resonance lines were measured with both directions of heater current and no shift was observed.

A possible source of error which must be considered is a shift of the fine-structure intervals due to atomic collisions (pressure shifts). We were unable to vary pressure over a sufficient range to attempt extrapolation to zero pressure. At high pressures, depolarization caused an intolerable loss of signal. At low pressures, the signal-to-noise ratio, based only on shot noise, became too small. All data, therefore, were taken at one pressure which could not be accurately measured, but almost certainly lay between 10 and 100 mTorr.

The pressure shift $\Delta\nu$ can be calculated by integrating the fine-structure frequency as a function of interatomic distance $\nu(R)$ times a probability function $P(R)$ over all space,

$$\Delta\nu = \int [\nu(R) - \nu_0] P(R) d^3R , \tag{14}$$

where ν_0 is the fine-structure frequency of the isolated molecule. Generally, $\nu(R)$ and $P(R)$ are difficult to determine, but we can estimate the order of magnitude of $\Delta\nu$ by assuming

$$\nu(R) = \begin{cases} (1+\epsilon)\nu_0 , & R < R' \\ \nu_0 , & R > R' \end{cases} \tag{15}$$

and

$$P(R) = Ne^{-V(R)/kT} \approx N \text{ atom/cm}^3, \tag{16}$$

where V is a potential function. The integral can now be evaluated and gives

$$\Delta\nu/\nu \approx \epsilon N \tfrac{4}{3}\pi (R')^3 . \tag{17}$$

If we take ϵ to be of the order of unity and R' to be the radius of the $4p$ electron, we obtain

$$\Delta\nu/\nu \approx 10^{-6} . \tag{18}$$

This estimate of the pressure shift is about two orders of magnitude smaller than the measurement errors, so we conclude that pressure shifts may be neglected.

Electric fields in the cavity could Stark shift the transition frequencies. There are two potentially important sources of electric field in this experiment. One is the relativistic electric field caused by the random motion of helium atoms through the magnetic field. The other is field penetration from the electron gun into the nominally equipotential cavity. A probable upper limit to both of these fields is 10 V/cm. From Bethe and Salpeter's[26] calculation of the Stark effect in He ($4\,^3P$), such a field should give a shift of less than 2 kHz. Consequently, Stark shifts may be neglected in comparison to the much larger measurement errors.

C. Linewidths

The minimum possible full width at half-height of a resonance line is the natural width $\Delta\nu$ which is determined by the radiative lifetime τ (in sec) according to

$$\Delta\nu = 1/\pi\tau . \tag{19}$$

Power broadening at the half-saturation point[1] introduces a factor of $\sqrt{2}$ into Eq. (19). If phase sensitive detection is used and a Lorentzian line shape is assumed, then maximum detection sensitivity is obtained when the modulation amplitude equals the linewidth[27] $\sqrt{2}\Delta\nu$. For this modulation amplitude, the separation between the maximum and minimum of the phase detected output (so-called first derivative presentation) is given by[27]

$$\nabla\nu' = \sqrt{3}(\sqrt{2}\Delta\nu) = \sqrt{6}\,\Delta\nu . \tag{20}$$

Experimentally, the magnetic field is varied rather than the frequency, so the peak separation is measured in gauss. Because the effective g value for all observed transitions is close to unity, the peak separation is given by

$$\Delta H = \Delta\nu'/g\mu_B = (5.5\times10^{-7}/\tau)\ \text{G} . \tag{21}$$

The radiative lifetimes for helium $3\,^3P$ and $4\,^3P$ are 1.05×10^{-7} and 1.5×10^{-7} sec, respectively,[28] so the expected peak separations are $\Delta H(3\,^3P) = 5.2$ G and $\Delta H(4\,^3P) = 3.7$ G. Although no extensive effort was made to measure linewidths (because of a low signal-to-noise ratio), the measured separations $\Delta H(3\,^3P) = 6.4 \pm 0.5$ G and $\Delta H(4\,^3P) = 6.7 \pm 0.5$ G are definitely larger than the expected peak separations. We believe that atomic collisions (pressure broadening) are the cause.

Pressure broadening is expected to be important when the time between state changing collisions is comparable to or shorter than the radiative lifetime. If we take the helium $4\,^3P$ cross section to be 200 Å^2 and the pressure to be 30 mTorr, a simple kinetic argument shows that the mean time between hard-sphere collisions of helium ($4\,^3P$) with ground-state helium is approximately 10^{-7} sec. This time is, indeed, comparable to the radiative lifetime. For the $3\,^3P$ state, which has a smaller radius, the time between collisions is increased by a factor of approximately 3. Consequently, the $3\,^3P$ transitions should be pressure broadened less than the $4\,^3P$ transitions. Experiment agrees with

TABLE II. Results.

$\Delta\nu_{01}$	$= 3306.6 \pm 1.0$ MHz
$\Delta\nu_{12}$	$= 270.7 \pm 0.8$ MHz
g_L	$= 0.999\,88 \pm 0.000\,03$
g_s	$= 2.002\,32$
χ_A	$= -0.080 \pm 0.016$ Hz/G

this conclusion.

Any atomic collisions which shorten the lifetime of a magnetic sublevel of the ^3P state will cause broadening of the microwave transitions. Collisional transitions within the ^3P state would likely be more frequent than those deexciting (quenching) the electronic state. Such behavior has been reported for the helium $2\,^3P$ state. Bennett *et al.*[28] give the deexcitation cross section as $<2\times10^{-16}$ cm^2, whereas Landman[29] gives the alignment depolarization cross section as $(5.6\pm0.2)\times10^{-15}$ cm^2, more than an order of magnitude larger. Thus we presume that the observed pressure broadening in the $4\,^3P$ state is caused by reorienting rather than deexciting collisions.

VI. DISCUSSION

A. Fine Structure

Our value for $\Delta\nu_{12}$ agrees with the value of Galleron-Julienne and Descoubes,[5(a)] 270.7 ± 0.2 MHz, but disagrees with the value of Maujean and Descoubes,[5(b),5(c)] and of Descoubes, 269.0 ± 0.1 MHz. The source of this discrepancy has not been determined. Our value for $\Delta\nu_{01}$ is about two orders of magnitude more precise than either of the previous values.[5] These results are included in Table III, which is a list of experimental fine-structure values for the helium $n\,^3P$ states.

An approximate calculation of the helium $n\,^3P$ fine structure,[30] based on the Breit equation and simple wave functions, shows that $n^3\Delta\nu_{01}$, $n^3\Delta\nu_{12}$, and $\Delta\nu_{01}/\Delta\nu_{12}$ should be constant. Experiment (Table III) confirms these relationships moderately well, but significantly large deviations occur at low n. This behavior is expected because the theory should be more accurate at large n.[30]

The approximate success of the theory suggests that it could be used to predict unmeasured fine-structure values. In addition, we suggest that the expected constancy of $n^3\Delta\nu_{01}$ and the accurate values for $n=2$–4 could be used to predict $\Delta\nu_{01}$ for $n>4$ to greater accuracy than the available experimental measurements.

B. Expectation Value of $r^2(4p)$

For the specific case of helium $4\,^3P$, Eq. (10) can be further simplified. The term involving the $1s$ electron may be dropped because the angular integral vanishes. Also the angular integral for the $M_L=\pm1$ states of a p electron is $-\frac{2}{5}$. Therefore,

$$\chi_A(4\,^3P)=-\frac{e^2}{10mc^2h}\,\langle 4\,^3P|r^2(4p)|4\,^3P\rangle\,, \qquad (22)$$

where χ_A is expressed in Hz/G^2. Finally,

$$\langle r^2(4p)\rangle = 190\pm38\ \text{Å}^2\,. \qquad (23)$$

This value agrees, within experimental error, with the corresponding value for a hydrogenic $4p$ orbital, 168 Å^2.

C. Quadrupole Moment

The atomic quadrupole moment may be defined as

$$Q_L=\langle L, M_L=L\,|\,\textstyle\sum_i er_i^2(3\cos^2\theta_i-1)\,|\,L, M_L=L\rangle\,. \qquad (24)$$

Comparison with Eq. (10) shows that

TABLE III. Experimental fine-structure intervals for helium $n\,^3$P.

n	Best experimental $\Delta\nu_{01}$ (MHz)	$\Delta\nu_{12}$ (MHz)	$\frac{\Delta\nu_{01}}{\Delta\nu_{12}}$	$n^3\Delta\nu_{01}$	$n^3\Delta\nu_{12}$
2	29 616.856 ± 0.060[a]	2291.196 ± 0.005[b]	12.9264 ± 0.0001	236 936 ± 1	18 329.6 ± 0.1
3	8113.78 ± 0.22[c]	658.55 ± 0.15[c]	12.321 ± 0.003	219 072 ± 6	17 781 ± 4
4	3306.6 ± 1.0[d]	270.7 ± 0.8[d]	12.21 ± 0.04	211 600 ± 60	17 325 ± 52
	3231 ± 500[e]	269.0 ± 0.1[e]	12.0 ± 1.9	207 000 ± 32 000	17 216 ± 6
	2970 ± 300[f]	270.7 ± 0.2[f]	11.0 ± 1.1	190 000 ± 19 000	17 325 ± 13
5	1415 ± 300[e]	135.5 ± 0.1[e]	10.4 ± 2.2	177 000 ± 38 000	16 940 ± 13
	1500 ± 200[f]			190 000 ± 25 000	
6	1123 ± 400[e]	77.27 ± 0.07[e]	14 ± 5	240 000 ± 86 000	16 690 ± 15
	860 ± 200[f]			190 000 ± 40 000	
7	•••	48.43 ± 0.15[e]	•••	•••	16 611 ± 51
8	268 ± 200[e]	32.49 ± 0.16[e]	8 ± 6	140 000 ± 100 000	16 635 ± 82
9	•••	22.8 ± 0.8[e]	•••	•••	16 600 ± 600

[a]Reference 8. [b]Reference 9. [c]Reference 3. [d]This work. [e]Reference 5(b). [f]Reference 5(a).

$$Q_L = [4mc^2L(2L-1)h/e]\chi_A$$
$$= (4530\times10^{-26})\chi_A$$
$$= -(360\pm70)\times10^{-26}\ \text{esu cm}^2, \quad (25)$$

where χ_A is expressed in Hz/G^2. This value agrees, within experimental error, with the value calculated for the hydrogen atom in its $4p$ state, -322×10^{-26} esu cm^2.

D. g_L Value

The value of g_L for the $4\,^3P$ state (Table II) is $0.999\,88\pm0.000\,03$, which may be compared to the theoretical value, $(1-m/M)=0.999\,86$. The difference between these two values is within experimental error, and cannot be taken too seriously. We should point out, however, that the calculation of the theoretical g_L has neglected the admixture of singlet and other triplet states into the $4\,^3P$ wave function. The importance of this effect should increase as the principal quantum number n increases and might alter g_L by 10 or 20 ppm for $n=4$. The spin-orbit and spin-spin coupling constants which determine the amount of such mixing are unknown, however, so it would be very difficult to improve the accuracy of the calculated g_L.

E. Future Experiments

We conclude by considering the capabilities and limitations of experiments similar to the one described above. As noted in the Introduction, the present study was initiated primarily to test apparatus design for microwave frequency spectroscopy of open-shell excited states of molecules. On the basis of these experiments we are now designing apparatus which we believe will lead to a hundredfold increase in signal to noise and make measurement accuracy an order of magnitude better. These improvements should make molecular experiments possible.

With the proposed apparatus the higher ^3P states of helium and similar states of other noble-gas atoms should also be accessible to measurement. Although such measurements would have *little* hope of ever providing a more accurate value of α than can be obtained from measurements on the $2\,^3P$ state of helium, the fine-structure parameters, g values, magnetic anisotropies, and quadrupole moments which could be determined would be of intrinsic value. They would be considerably more precise than values calculated from *ab initio* wave functions and hence could serve as tests of such wave functions. In a less precise way, measurements on a series of states could provide deeper insight to the nature of Rydberg states.

Finally, it appears that linewidth measurements could be used to study reorienting collisions between Rydberg states and ground-state atoms. Apparently many such collisions can take place before deactivation of the excited state. It should be most interesting and useful to study the details of these processes and measure their cross sections.

ACKNOWLEDGMENTS

We would like to thank M. Leventhal and J. Gersten for helpful discussions and B. Zegarski for taking many of the data.

[1]W. E. Lamb, Jr., Phys. Rev. 105, 559 (1957).
[2]W. E. Lamb, Jr. and T. H. Maiman, Phys. Rev. 105, 573 (1957).
[3]I. Wieder and W. E. Lamb, Jr., Phys. Rev. 107, 125 (1957).
[4]J. Lifsitz and R. H. Sands, Bull. Am. Phys. Soc. 10, 1214 (1965).
[5](a) C. Galleron-Julienne and J. P. Descoubes, Compt. Rend. 261, 916 (1965); (b) M. Maujean and J. P. Descoubes, *ibid.* 264, 1653 (1967); (c) J. P. Descoubes, in *Physics of the One- and Two- Electron Atoms*, edited by F. Bopp and H. Kleinpoppen (North-Holland, Amsterdam, 1969), p. 341.
[6]F. M. J. Pichanick, R. D. Swift, C. E. Johnson, and V. W. Hughes, Phys. Rev. 169, 55 (1968).
[7]C. E. Johnson, F. M. J. Pichanick, A. Kponou, S. A. Lewis, and V. W. Hughes, Bull. Am. Phys. Soc. 13, 20 (1968).
[8]A. Kponou, V. W. Hughes, C. E. Johnson, S. A. Lewis, and F. M. J. Pichanick, Bull. Am. Phys. Soc. 15, 488 (1970).
[9]S. A. Lewis, F. M. J. Pichanick, and V. W. Hughes, Phys. Rev. A 2, 86 (1970).
[10]V. W. Hughes, in *Atomic Physics*, edited by V. W. Hughes, B. Bederson, V. W. Cohen, and F. M. J. Pichanick (Plenum, New York, 1969), p. 15.
[11]C. L. Pekeris, B. Schiff, and H. Lifson, Phys. Rev. 126, 1057 (1962).
[12]B. Schiff, C. L. Pekeris, and H. Lifson, Phys. Rev. 137, 1672 (1965); B. Schiff, H. Lifson, C. L. Pekeris, and P. Robinowitz, *ibid.* 140, 1104 (1965).
[13]C. Schwartz, Phys. Rev. 134, A1181 (1964).
[14]C. Schwartz, in Ref. 10, p. 71.
[15]F. A. Jenkins and E. Segrè, Phys. Rev. 55, 52 (1939).
[16]L. I. Schiff and H. Snyder, Phys. Rev. 55, 59 (1939).
[17]D. Harting and P. F. A. Klinkenberg, Physica 14, 669 (1949).
[18]W. B. Garn, R. S. Caird, D. B. Thomson, and C. M. Fowler, Rev. Sci. Instr. 37, 762 (1966).
[19]W. Hüttner and W. H. Flygare, J. Chem. Phys. 47, 4137 (1967); W. Hüttner, M.-K. Lo, and W. H. Flygare, *ibid.* 48, 1206 (1968); W. H. Flygare, W. Hüttner, R. L. Shoemaker, and P. D. Foster, *ibid.* 50, 1714 (1969).
[20]J. R. P. Angel, P. G. H. Sandars, and G. K. Woodgate, J. Chem. Phys. 47, 1552 (1967).
[21]M. Phillips, Phys. Rev. 88, 202 (1952).
[22]A. Abragam and J. H. Van Vleck, Phys. Rev. 92, 1448 (1953).

[23]C. P. Poole, *Electron Spin Resonance* (Interscience, New York, 1967).

[24]D. MacNair, IEEE J. Quantum Electron. QE5, 460 (1969).

[25]The standard error of a parameter i is defined as $C_{ii}[\Phi/(n-K)]^{1/2}$, where Φ is the minimized sum of the squares of the residuals, n is the number of data points, K is the number of parameters, and C_{ii} is the ith diagonal element of the inverse matrix of the normal equation matrix.

[26]H. A. Bethe and E. E. Salpeter, *Quantum Mechanics of One-And-Two-Electron Atoms* (Springer, Berlin, 1957), p. 241.

[27]H. Wahlquist, J. Chem. Phys. 35, 1708 (1961).

[28]W. R. Bennett, Jr., P. J. Kindlmann, and G. N. Mercer, Appl. Opt. Suppl. No. 2, 34 (1965).

[29]D. A. Landman, Phys. Rev. 173, 33 (1968).

[30]Reference 26, p. 183.

PHYSICAL REVIEW A VOLUME 4, NUMBER 1 JULY 1971

Screening of Many-Electron Atoms*

Carl A. Rouse

Gulf General Atomic, Incorporated,† San Diego, California 92112

(Received 20 July 1970; revised manuscript received 11 January 1971)

The problem of the screening of many-electron atoms (ions) is considered. Using the scaled Thomas-Fermi (STF) method of Stewart and Rotenberg for approximating the core potential of an atom (ion) with nuclear charge Z and net core charge Z^*, a screened scaled Thomas-Fermi potential (SSTF) is presented: $V(r) = -(Ze^2/r)\,U_{\mathrm{SSTF}}$, where

$$U_{\mathrm{SSTF}} = U(r) - Ar, \qquad 0 \le r \le a$$
$$= BU(r)\,e^{(a-r)/D}, \qquad r \ge a.$$

Here D is the screening radius; A and B are constants; and $U(r)$ is given by

$$U(r) = U_{\mathrm{STF}}(r) = \varphi(r/\alpha\mu) + qr/r_c, \qquad r \le r_c$$
$$= q, \qquad r \ge r_c$$

where $\varphi(r/\alpha\mu)$ is the well-known Thomas-Fermi function, r_c is the STF core radius with $\mu = \frac{1}{4}(9\pi^2/2Z)^{1/3} = 0.88534Z^{-1/3}$, α is the adjustable scaling factor, and $q = Z^*/Z$. The constants B and A are given by $B = D[aU'(a) - U(a)]/\{D[aU'(a) - U(a)] - aU(a)\}$ and $A = (1-B)\,U(a)/a$, where $U'(a) = \partial U/\partial r$ at $r = a$. Eigenvalues of the Schrödinger equation with the SSTF potential are given for the $3d$, $4s$, $4p$, $4d$, $4f$, and $5s$ orbitals of Fe I and Fe VIII. Comparisons between the ions and corresponding hydrogenic orbitals show that the variations of the SSTF eigenvalues and the limiting screening radii are generally very different, with different level crossings and different relative energies. It is concluded that in order to obtain a correlation between a limiting screening radius and the observed disappearance of lines from a many-electron atom (ion), SSTF solutions are needed for the ion of interest. It is also concluded that until an accurate external screening function is obtained and applied to the screening of Hartree-Fock isolated-atom (-ion) solutions, SSTF solutions will be useful for the very important astrophysical problems of calculating equations of state and opacities for high-Z matter at stellar densities and temperatures.

I. INTRODUCTION

In this paper we consider the screening of bound orbitals of many-electron atoms (ions) by neighboring particles. Previous studies[1-12] have analyzed the screening of bound orbitals of one-electron hydrogenic ions with a point nuclear charge Z; in considering ions with two or more bound electrons, the core is assumed to be a point with an effective charge $Z^* = Z - N_b + 1$, where N_b is the number of bound electrons. (In this paper $N_b \le Z$.) The reasons for using hydrogenic assumptions are obvious. In view of the considerable effort needed to accurately understand isolated many-electron atoms (ions) with the self-consistent-field methods of Hartree[13(a)] and Slater,[13(b)] it is hardly feasible to consider accurate solutions with the additional interactions of neighboring atoms, ions, and free electrons in matter at finite densities and nonzero temperatures—systems that are further complicated by the dynamic time-dependent quality of even an equilibrium plasma.

Nevertheless, the hydrogenic screened Coulomb solutions of the time-independent Schrödinger equation have been of value in gaining a crude approximation to the many-electron-atom screening problem. As the next step in this problem, this paper will formulate a better approximation to the screening of many-electron atoms by considering the external screening of an atomic orbital. The electron